The Radiation Environment on-board the International Space Station

Oscar Larsson
Royal Institute of Technology

March 12, 2013

Outline

The Discovery of Cosmic Rays

- 7 August 1912 V. Hess
  "The results of my observation are best explained by the assumption that a radiation of very great penetrating power enters our atmosphere from above."
- Nobel Price 1936
- MSL-RAD coincidence?

Image from Wikipedia

100 YEARS OF COSMIC RAY RESEARCH

- 1932 e^+ C.D. Andreson
- 1949 Fermi Cosmic ray acceleration
- 1958 ”van Alen Belts”
- 1966 CMB 2.7 K
- Beginning of 1990 $2 - 3 \cdot 10^{20} eV$

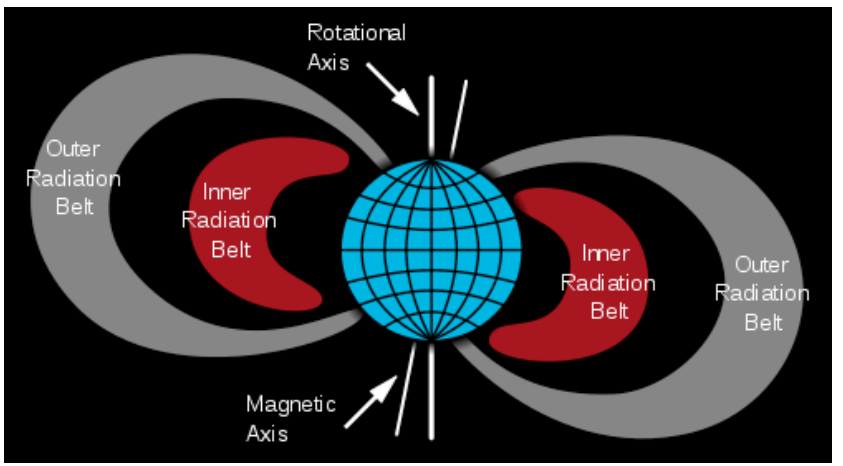

Image from Wikipedia

COMPOSITION OF THE COSMIC RAY SPECTRUM

Particle Composition

- p, e, and He: 99%
- 1% Heavy ions
- Origin? Acceleration?

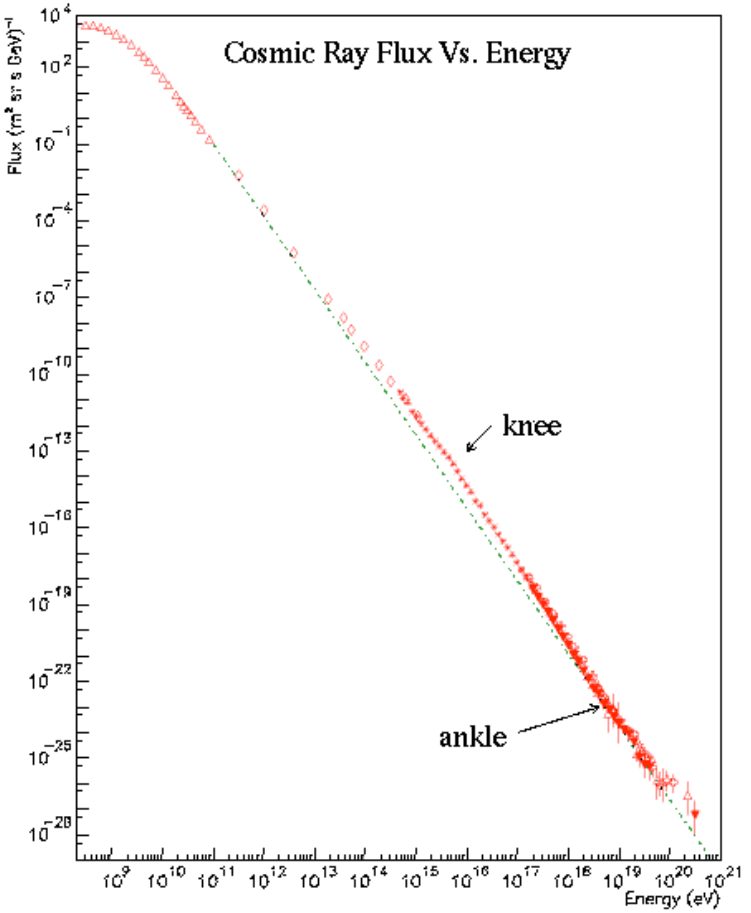

Image from lanl.gov

Origin of Galactic Cosmic Rays

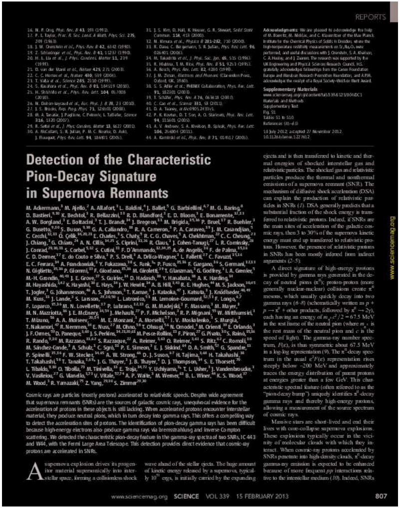
REPORTS

Detection of the Characteristic Pion-Decay Signature in Supernova Remnants

Cosmic rays are particles (mostly protons) accelerated to relativistic speeds. Despite wide agreement that supernova remnants (SNRs) are the sources of galactic cosmic rays, unequivocal evidence for the acceleration of protons in these objects is still lacking. When accelerated protons encounter interstellar material, they produce neutral pions, which in turn decay into gamma rays. This offers a compelling way to detect the acceleration sites of protons. The identification of pion-decay gamma rays has been difficult because high-energy electrons also produce gamma rays via bremsstrahlung and inverse Compton scattering. We detected the characteristic pion-decay feature in the gamma-ray spectra of two SNRs, IC 443 and W44, with the Fermi Large Area Telescope. This detection provides direct evidence that cosmic-ray protons are accelerated in SNRs.

A supernova explosion drives its progenitor material supersonically into interstellar space, forming a collisionless shock wave ahead of the stellar ejecta. The huge amount of kinetic energy released by a supernova, typically 10^{51} ergs, is initially carried by the expanding

www.sciencemag.org SCIENCE VOL 339 15 FEBRUARY 2013 807

The Fermi collaboration published on 15 Feb

- The Origin of CR
- Acceleration of p

In principal:
$p + p \rightarrow \pi^0 + X$
In 99%: $\pi^0 \rightarrow 2\gamma$

THE 1%

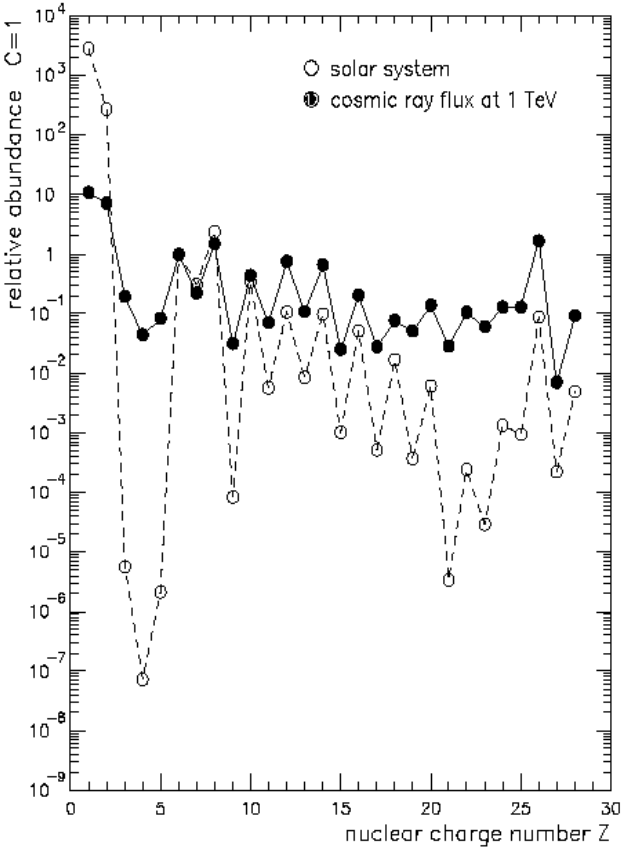

Image taken from Simpson 1983

The Composition of Heavy Nuclei

- $\frac{dE}{dx} \propto z^2$
- Fe$\approx$ 0.02 %
  $\rightarrow$ 20-50 % D_{eq}

(D_{eq} = Equivalent dose)

The Health Risk

The ability to *a priori* accurately predict health risks is paramount for the future of space exploration.

The International Space Station

Complications due to Composition

Modulation factors

- Hull Thickness
- Hull Composition
- Rack Configuration
- Other interior stuff

Image from NASA

Monitoring the Radiation Environment

The Matroshka Dosimeter

Different Detectors

- SilEye-3/Alteino
- AMS
- Passive dosimetry
  TEPC, CR-39 etc.

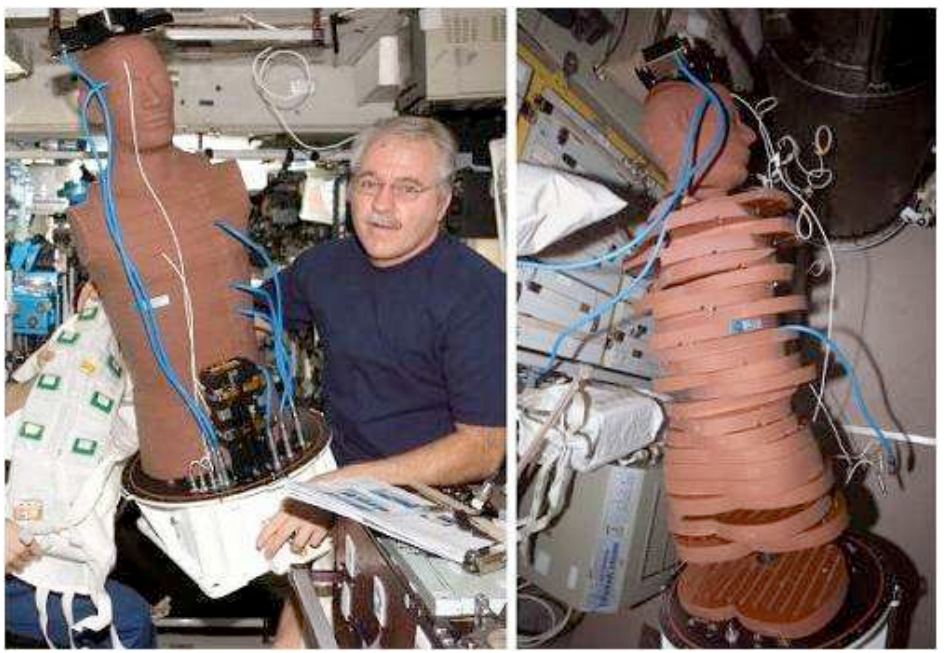

The SilEye-3/Alteino Experiment

Detector characteristics

- 8 Silicon Planes
- 32 Strips/Plane
- Particle Abundance
- Shielding effect
- Dose measurement
- Fragmentation analysis

Image NASA

Relative Abundance

Relative Abundance in the Russian Pirs module

Equivalent Aluminium

Modulated ratio of particle abundance:

$$P(Fe \rightarrow X) = \frac{\sigma_X N_A}{M_{Al}} \cdot \rho_{Al} \Delta x \tag{1}$$

$$Fe/X = \frac{N_{Fe0}(1 - P(Fe \rightarrow All))}{(N_{X0} + N_{Fe0} P(Fe \rightarrow X))} \tag{2}$$

N_{Fe0} and N_{X0} are number density outside the ISS.

Equivalent Aluminium

Calculating Hull Thickness by Epax 2.1 and Geant4 QGSP_BIC

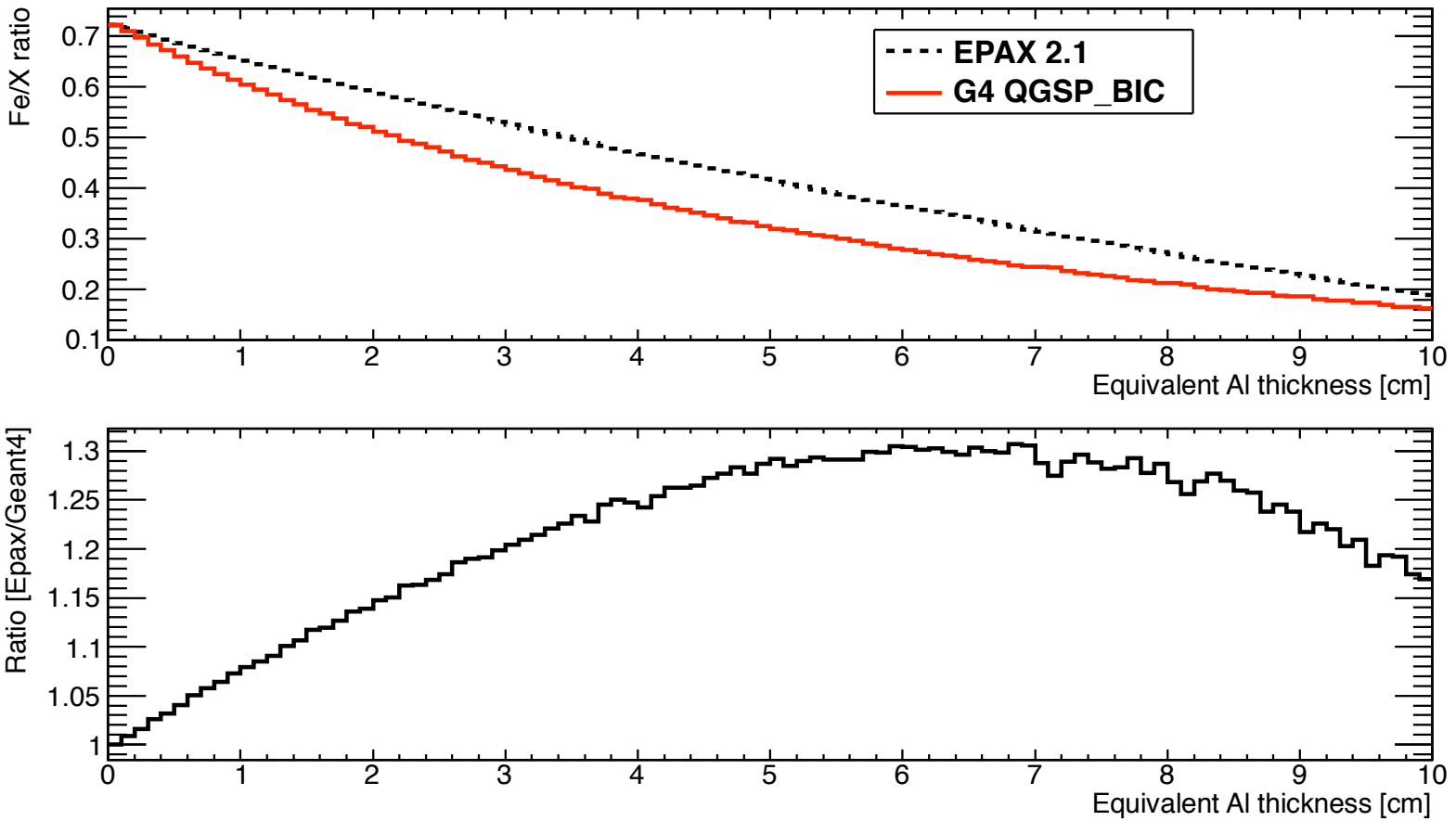

Dose and Equivalent Dose Rates

Effects of data analysis cuts

Data Cuts

- Angular
- Multiplicity
- Energy

Dose and Equivalent Dose Rates

Conversion from LET_{Si} to LET_{H_2O} has traditionally been done by constant factor.

We use

$$Log(LET_{H_2O}) = -0.2902 + (1.025 \cdot Log(LET_{Si})) \tag{3}$$

E.R Benton et. al, Radiation Measurements, 45, 2010, 957-959

Dose and Equivalent Dose Rates

Data

- SilEye-3/Alteino
- ALTEA
- Dostel (MIR)
- CR-39 (JAXA)

Dose and Equivalent Dose Rates

Multiplicity distribution of events are well confined however the contribution to D_r and D_{eq} aren't as well confined.

Summary

The results from SilEye-3/Alteino to date

- Clear increase in flux of odd charged particles
- Shielding efficiency of Polyethylene
- Particle flux non-isotropic
- Dose and Dose rates are consistent and isotropic

Outlook

For SilEye-3/Alteino

- Analysis of high multiplicity events
- δ_e production in data vs Monte Carlo (Geant4)
- Continuing mapping the radiation environment

General issues for the assessment of radiation risks

- Several different Monte Carlo codes
- Multiple physics list
- Geometry description

Outlook

The risks in long duration and/or deep space space missions due to radiation needs to be dealt with in order to continue with such explorations.

Thank You for your Attention!

SRS
Organising Committee

Questions?

Image source, unknown

Back Up

Alteino Detector Description

SilEye-3/Alteino

- 8 planes, 8x8 cm^2, 380 μm
- $Gf \approx 24 cm^2 sr$
- Readout electronics based on Pamela
- 16 bit ADC
- Calibration 3.3 keV/ADC_{ch}
- Max $dE \approx 174$ MeV

Image from http://wizard.roma2.infn.it/sileye/index.htm

Alteino Data Cuts

Angular normalisation

- $cos(\theta_{inc})$

Multiplicity

- LET: MSA $<$ 200 (256)
- ST: MSA $<$ 32 (256)

Kinetic Energy

$$\left| \frac{(E_1 + E_2) - (E_7 + E_8)}{(E_1 + E_2) + (E_7 + E_8)} \right| < 20\% \tag{4}$$

LET conversion, Benton et. al

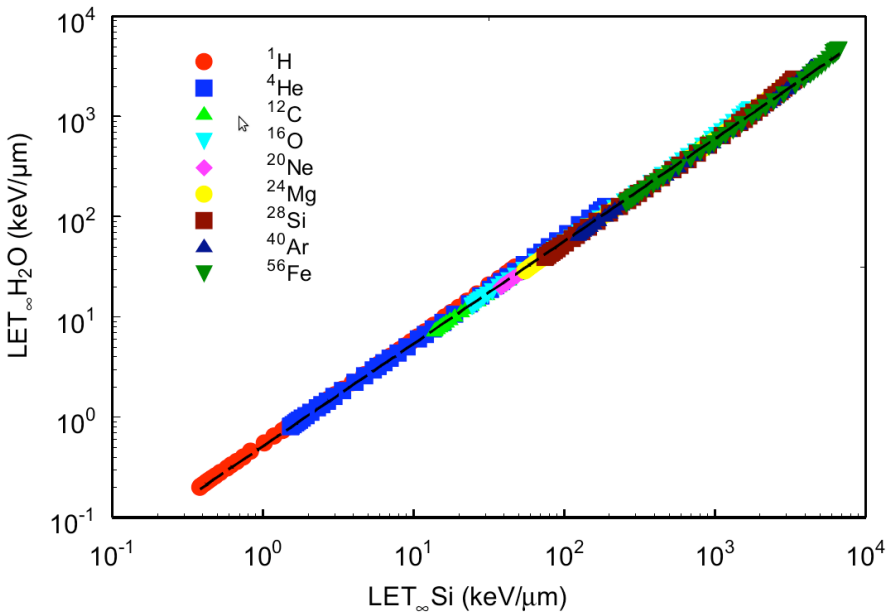

MISSION TO MARS

18 Pages Feasibility study

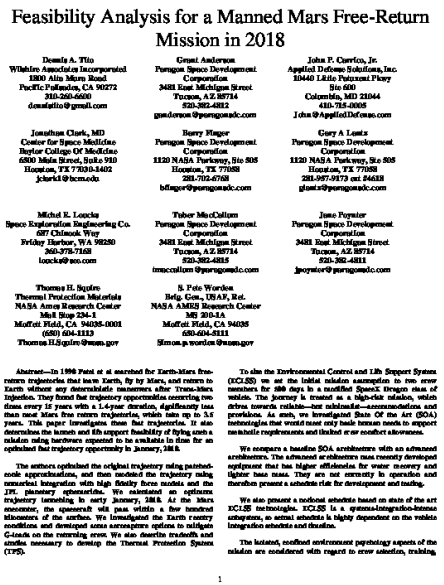

Feasibility Analysis for a Manned Mars Free-Return Mission in 2018

Dennis A. Tito
Wilshire Associates Incorporated
1900 Alta Mesa Road
Pacific Palisades, CA 90272
310-260-6600
denistito@gmail.com

Gene Anderson
Paragon Space Development Corporation
3481 East Michigan Street
Tucson, AZ 85714
520-382-4812
ganderson@paragonsdc.com

John P. Carrico, Jr.
Applied Defense Solutions, Inc.
10440 Little Patuxent Pkwy
Ste 600
Columbia, MD 21044
410-715-0005
John@AppliedDefense.com

Jonathan Clark, MD
Center for Space Medicine
Baylor College Of Medicine
6800 Main Street, Suite 910
Houston, TX 77030-1402
jclark1@bcm.edu

Barry Finger
Paragon Space Development Corporation
1120 NASA Parkway, Ste 505
Houston, TX 77058
281-702-6768
bfinger@paragonsdc.com

Gary A Lantz
Paragon Space Development Corporation
1120 NASA Parkway, Ste 505
Houston, TX 77058
281-957-9173 ext 84633
glantz@paragonsdc.com

Michel E. Loucks
Space Exploration Engineering Co.
687 Chinook Way
Friday Harbor, WA 98250
360-378-7168
loucks@eec.com

Taber MacCallum
Paragon Space Development Corporation
3481 East Michigan Street
Tucson, AZ 85714
520-382-4815
tmaccallum@paragonsdc.com

Jane Poynter
Paragon Space Development Corporation
3481 East Michigan Street
Tucson, AZ 85714
520-382-4811
jpoynter@paragonsdc.com

Thomas H. Squire
Thermal Protection Materials
NASA Ames Research Center
Mail Stop 234-1
Moffett Field, CA 94035-0001
(650) 604-1113
Thomas.H.Squire@nasa.gov

S. Pete Worden
Brig. Gen., USAF, Ret.
NASA AMES Research Center
MS 200-1A
Moffett Field, CA 94035
650-604-5111
Simon.p.worden@nasa.gov

Abstract—In 1996 Patel et al searched for Earth-Mars free-return trajectories that leave Earth, fly by Mars, and return to Earth without any deterministic maneuvers after Trans-Mars Injection. They found fast trajectory opportunities occurring two times every 15 years with a 1.6-year duration, significantly less than most Mars free return trajectories, which take up to 3.5 years. This paper investigates these fast trajectories. It also describes the human and life support feasibility of flying such a mission using hardware expected to be available in time for an optimized fast trajectory opportunity in January, 2018.

The authors optimized the original trajectory using patched-conic approximations, and then modeled the trajectory using numerical integration with high fidelity force models and the JPL planetary ephemerides. We calculated an optimum trajectory launching in early January, 2018. At the Mars encounter, the spacecraft will pass within a few hundred kilometers of the surface. We investigated the Earth reentry conditions and developed some aerocapture options to mitigate G-loads on the returning crew. We also describe tradeoffs and studies necessary to develop the Thermal Protection System (TPS).

To size the Environmental Control and Life Support System (ECLSS) we set the initial mission assumption to two crew members for 880 days in a modified SpaceX Dragon class of vehicle. The journey is treated as a high-risk mission, which drives towards reliable—but minimalist—accommodations and provisions. As such, we investigated State Of the Art (SOA) technologies that would meet only basic human needs to support metabolic requirements and limited *in situ* comfort allowances.

We compare a baseline SOA architecture with an advanced architecture. The advanced architecture uses recently developed equipment that has higher efficiencies for water recovery and lighter base mass. They are not currently in operation and therefore present a schedule risk for development and testing.

We also present a notional schedule based on state of the art ECLSS technologies. ECLSS is a systems-integration-intense subsystem, so actual schedule is highly dependent on the vehicle integration schedule and timeline.

The lowest, excellent environment psychology aspects of the mission are considered with regard to crew selection, training,

"In addition to spacecraft materials of construction, radiation protection is provided by a water shield made up of water in storage for other subsystems."
"Further studies needs to be done to find creative solutions for radiation protection, [...]"